

4 The Cool ISM in Galaxies

Jan M. van der Hulst¹ · W. J. G. de Blok²

¹Radio Astronomy, Kapteyn Astronomical Institute, University of Groningen, Groningen, The Netherlands

²Astronomy Group, ASTRON, Netherlands Foundation for Radio Astronomy, Dwingeloo, The Netherlands

1	<i>Introduction</i>	184
2	<i>The Neutral Hydrogen (H I) in Galaxies</i>	185
2.1	The H I Physics and Observables	185
2.2	The Distribution of H I in Galaxies	188
2.3	The Warm and Cold ISM in Galaxies	192
3	<i>Star Formation and the ISM</i>	193
4	<i>Accretion, Feedback and the Environment</i>	199
	<i>References</i>	202

Abstract: This chapter describes the different constituents of the observable interstellar medium (ISM) in galaxies and reviews the relationships between the ISM and the star formation in galaxies. The emphasis is on the component which is most widespread and most easily observable, the neutral atomic hydrogen (H I). It briefly touches upon effects of the environment and of the interplay between star formation and the ISM (feedback).

1 Introduction

The best census of the different components of the interstellar medium (ISM) exists for the Milky Way, the result of close to half a century of observational and theoretical studies. Much of this is well described in various chapters of the Handbook (🔗 [Chap. 10](#) of Volume 5). The ISM components range from various forms of the most abundant species, neutral hydrogen (H I), ionized hydrogen (H II), and molecular hydrogen (H₂), and a large variety of complex molecules and dust grains, to the more energetic components of the cosmic ray population. In this chapter, we restrict ourselves to the neutral hydrogen component of the ISM in galaxies and only briefly address some of the other components such as the ionized and molecular hydrogen, and the dust.

The ISM plays a crucial role in the process of star formation throughout a galaxy's lifetime. How efficiently star formation proceeds depends on the local properties of the ISM. These are in turn affected by the star formation which provides feedback via stellar winds and supernova explosions. This feedback is an important regulating mechanism for the ongoing process of the buildup of galaxies throughout cosmic time. Detailed imaging of the ISM, in particular in H I is now available for many objects in the nearby universe. This chapter will therefore briefly review the current ideas and observational evidence for the physical connection between the local properties of the ISM and the star formation.

Although such constituents of the ISM as dust and ionized gas have long been known in the Galaxy, it was not until the detection of the first 21-cm line emission of H I (Ewen and Purcell 1951; Muller and Oort 1951; Pawsey 1951), following the prediction by van de Hulst (1945), opened a full perspective on the structure, kinematics, and physics of the H I in the Galaxy (see 🔗 [Chap. 11](#) of Volume 5). The first pioneering observations of H I in other galaxies (Raimond and Volders 1957; Volders 1959; Volders and Högbom 1961) were the beginning of several decades of galaxy surveys in the H I line using single-dish radio telescopes of increasing diameter. This led to insight into the global properties of H I in galaxies, well summarized in Roberts and Haynes (1994) following the much earlier reviews of Roberts (1963, 1975).

The advent of earth-rotation synthesis radio telescopes drastically changed the field, as it became possible to image the H I in galaxies with angular resolutions of a few arcminutes originally (Baldwin et al. 1971; Rogstad and Shostak 1971; Wright et al. 1972) with quality improving over the years to $\sim 5''$ (Walter et al. 2008). By 2012 some 500 galaxies have been imaged in the H I line, some individually, some as part of large observing programs such as WHISP (van der Hulst et al. 2001; García-Ruiz et al. 2002; Swaters et al. 2002; Noordermeer et al. 2005) and THINGS (Walter et al. 2008). Although a main focus of the earlier work was on using the H I kinematics to determine the mass distributions of galaxies, in particular the dark matter content (Sanders 2010), this chapter will primarily discuss the distribution of the H I in relation to other components of the ISM, and in particular in relation to the star formation in galaxies, using the latest results from surveys such as WHISP and THINGS in H I, and BIMA-SONG (Helfer et al. 2003) and HERACLES (Leroy et al. 2008, 2009) in CO.

This chapter will not repeat the information of many previous reviews, nor will it review recent low-resolution surveys of H I in galaxies such as HIPASS (Meyer et al. 2004; Zwaan et al. 2004; Koribalski et al. 2004) or ALFALFA (Giovanelli et al. 2005; Toribio et al. 2011). It will concentrate instead on the resolved distribution of the ISM as traced by the H I, as there now is a wealth of information from high-resolution H I imaging of a few hundred galaxies. Furthermore, it will discuss the relation of the H I and other ISM components to the star formation in galaxies and touch upon the role of the star formation and the environment in shaping the distribution of the H I. This chapter provides an overview of the current knowledge of the cool ISM and its relation to star formation in galaxies, but does not pretend to be complete.

2 The Neutral Hydrogen (H I) in Galaxies

This section first provides a brief discussion of the relevant physics of the H I and associated observables, followed by an overview of the detailed distribution of H I in galaxies, and a brief description of the warm and cold components of the ISM.

2.1 The H I Physics and Observables

The basic physics of the H I atom is well described in [Chap. 11](#) of Volume 5 and in Walterbos and Braun (1996). A full treatment of the level population of the hydrogen atom is given in Field (1959). In the ISM, collisions dominate the excitation of the fine-structure 21-cm H I line. Resolved observations of H I in galaxies provide a set of images of the H I at a series of frequencies (i.e., Doppler velocities) determined by the spectral resolution and observing frequency used. Each image basically provides the brightness distribution of the H I line at a particular Doppler velocity. For each line of sight then an H I profile can be constructed which can be integrated over all velocities to determine a column density. The realization that the H I in galaxy disks is predominantly optically thin allows us to determine H I column densities directly from the measured brightness temperatures of the H I emission using the following equation:

$$\frac{N_{\text{HI}}}{\text{cm}^{-2}} = 1.823 \times 10^{18} \int \frac{T_B(v)}{\text{K kms}^{-1}} dv, \quad (4.1)$$

where the brightness temperature $T_B(v)$ is related to the flux per beam ($S(v)$, the usual units used in synthesis maps) and the beam area (Ω_B) via

$$T_B(v) = 606(\lambda/21.1\text{cm})^2 \frac{S(v) \text{ (mJy)}}{\Omega_B \text{ (sq.arcsec)}} \quad (4.2)$$

The column density basically is the integral over velocity of all emission along a given line of sight within one resolution element. Commonly, it is determined by calculating the 0th moment of the measured H I profiles. Higher order moments can also be calculated and are a measure of a characteristic radial velocity (1st moment) and velocity dispersion (2nd moment). These higher order moments are not necessarily the best measures of velocity and velocity dispersion. Better results are obtained by fitting profiles with a single or multiple Gaussians or Gauss-Hermite polynomials (Noordermeer et al. 2005; Swaters et al. 2002).

In addition to determining observational parameters of each line of sight, one can also integrate the H I signal spatially to determine the total flux in each channel for a given object

(e.g., an entire galaxy, a companion feature, or a feature within a galaxy disk). These fluxes can be integrated over velocity to determine the total mass, which is related to the total flux integral as

$$\frac{M_{\text{HI}}}{M_{\odot}} = 236 \left(\frac{D}{\text{Mpc}} \right)^2 \int \frac{S(\nu)}{\text{mJy}} \frac{d\nu}{\text{kms}^{-1}} \quad (4.3)$$

When calculating detection limits based on the rms noise of the observation, one has to assume a profile velocity width as both N_{HI} and M_{HI} are integrated over velocity. This has led to a range of limit definitions in the literature as some authors integrate over the velocity resolution while others use (different) estimates of the expected profile width for the objects under study. It would be better to introduce uniformity and quote limits in $N_{\text{HI}}/\Delta\nu$ and $M_{\text{HI}}/\Delta\nu$ rather than N_{HI} and M_{HI} to avoid this practical problem.

For HI absorption, the situation is more complex as HI absorption measurements basically probe optical depth:

$$\tau(\nu) = 5.49 \times 10^{-14} \frac{N_{\text{HI}}}{T_s} P(\nu) \quad (4.4)$$

with a Maxwellian velocity distribution $P(\nu)$ given by

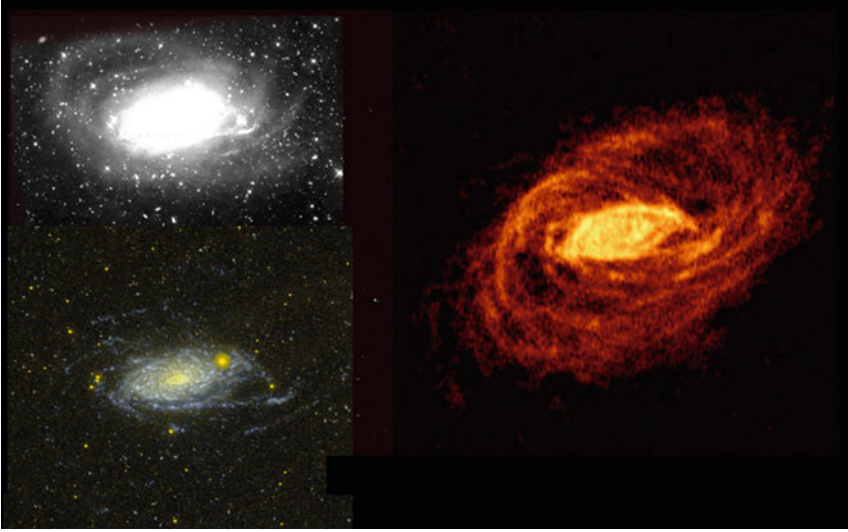
$$P(\nu) = \frac{1}{\sqrt{\pi} \cdot b} e^{(-\nu/b)^2} \quad (4.5)$$

with

$$b = \sqrt{\frac{2kT_k}{m_{\text{HI}}}}, \quad (4.6)$$

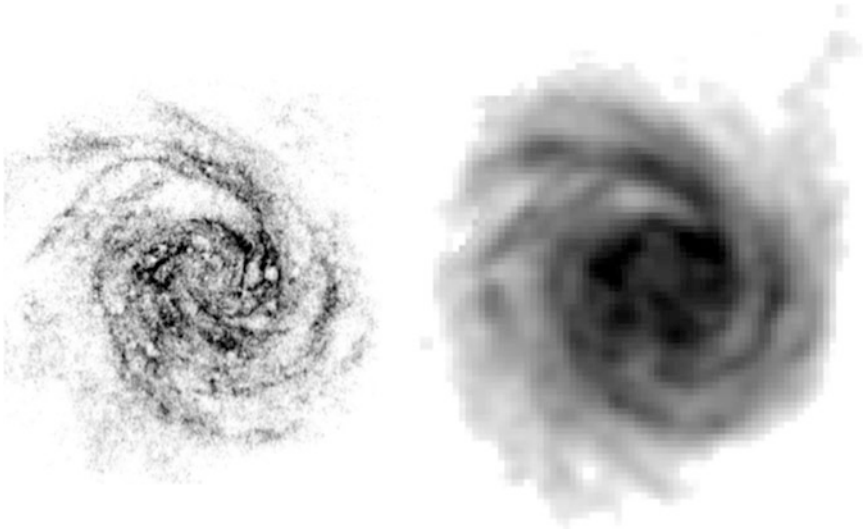
where $\tau(\nu)$ is the optical depth and T_s and T_k are the spin temperature and the kinetic temperature of the HI, respectively. Because the optical depth depends on both the column density (N_{HI}) and the spin temperature, it is not possible to interpret absorption line measurements unambiguously. This is a major limitation which can only be resolved if one has an independent measurement of HI emission along the same line of sight. For small optical depths, the absorption and emission observations can be combined to solve for N_{HI} and T_s independently. Such observations do not generally exist, however, so an assumption about the spin temperature is required to estimate column densities from absorption line measurements.

An example of the HI distribution of a spiral galaxy is given in [Fig. 4-1](#). It shows NGC 5055 in HI, visible light, and UV (GALEX). The HI reveals a wealth of structure, not only in the inner part of the galaxy, coincident with the bright optical disk, but also in the outer parts where faint light is present and structures in UV light indicate the presence of star formation. This HI observation is rather deep. Most HI synthesis observations in the literature do not probe much deeper than column densities of $N_{\text{HI}} \sim 10^{20} \text{cm}^{-2}$ for the typical sensitivities and angular resolutions used. Synthesis observations offer the flexibility of improving the column density sensitivity by changing the weights of the u, ν data. Giving lower weight to the longer baselines lowers the resolution (increases Ω_B) and enhances the surface brightness sensitivity and hence column density sensitivity. This is illustrated further in [Fig. 4-2](#) which shows the HI distributions of NGC 6946 at two resolutions: $6''$ and $60''$. It is clear that the $60''$ image brings out fainter features at the expense of resolution, especially in the outer parts. Most notable is the faint tail in the northwest which is interpreted as the remnant of an infalling gas complex (Boomsma et al. 2008). These images result from long integrations at the Very Large Array (VLA) and Westerbork Synthesis Radio Telescope (WSRT).



■ Fig. 4-1

Deep optical (Martínez-Delgado et al. 2010), GALEX UV (Thilker et al. 2007), and WSRT H I (Battaglia et al. 2005) images of the warped galaxy NGC 5055. The H I intensities range from a limiting column density of about $3 \times 10^{19} \text{ cm}^{-2}$ to a peak of $1 \times 10^{21} \text{ cm}^{-2}$ (Note the extent of the H I but also the presence of faint optical features and star formation in the outer parts with its wealth of structure)



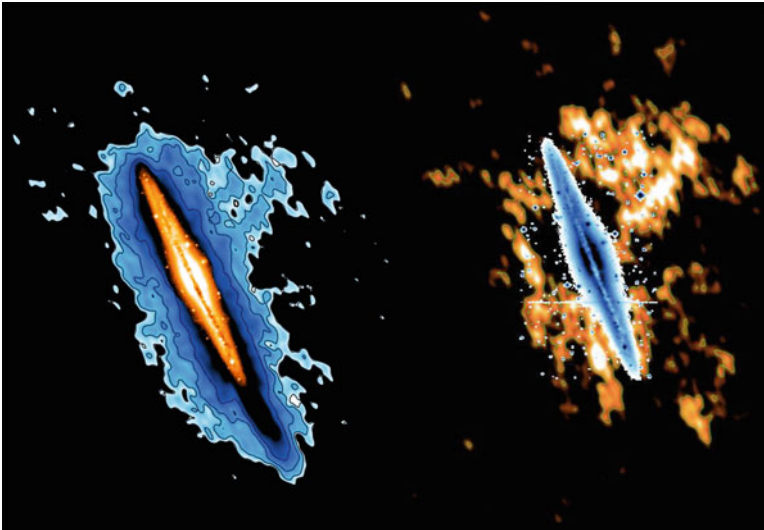
■ Fig. 4-2

H I images of the galaxy NGC 6946 at two different resolutions. *Left panel:* 6'' resolution VLA data from THINGS (Walter et al. 2008). *Right panel:* 60'' resolution WSRT data from Boomsma et al. (2008) (Note the faint extension in the northwest, possibly a recent accretion event)

2.2 The Distribution of H I in Galaxies

Observations of H I in other galaxies have clearly confirmed the picture that emerged from studies of the Milky Way: most of the H I is in a thin (\sim few hundred pc scale height), rotating disk, typically more extended radially than the observable distribution of star light. This disk may flare and warp in the outer parts as does the H I disk of the Milky Way (Levine et al. 2006; Kerr 1969, and references therein). In addition, evidence is mounting for the presence of extraplanar H I: either gas thrown out of the disk by star formation activity (the “Galactic Fountain,” Bregman 1980), or gas accreted from satellite galaxies (such as the Magellanic Stream around the Milky Way, Putman et al. 2003) or from the cosmic web (Sancisi et al. 2008). Edge-on galaxies provide the best view of both the thin H I disk and such extraplanar H I. Prominent, well-studied examples are NGC 891 and NGC 4565 (Oosterloo et al. 2007a; Rupen 1991). In NGC 891, observations of increasing depth provided the first evidence for extraplanar H I. Part of this H I is in a more slowly rotating, thick disk reaching scale heights of a few kpc; another part consists of more patchy filaments, reaching heights of 10 kpc above the plane, and is kinematically less well behaved. These components are illustrated in [Fig. 4-3](#) and will be discussed in more detail later.

The overall radial surface density (i.e., deprojected column density) distribution of H I in the disks of spiral galaxies is rather flat within the optical disk, with an approximately exponential decline in the outer parts (Swaters et al. 2002; Bigiel et al. 2008). Early-type spiral galaxies tend to have a deficiency of H I surface density in the inner parts, often compensated by the presence of large amounts of H₂ (Noordermeer et al. 2005). Typical average surface densities



■ Fig. 4-3

Deep WSRT H I images of NGC 891 (Oosterloo et al. 2007a). *Right panel* shows the integrated H I image superposed on the optical image of the galaxy. At this resolution and sensitivity, the thick, lopsided H I distribution is very clear. The *right panel* shows only the H I that is not corotating with the disk. This anomalous-velocity gas is everywhere, but most prominent and extended in the northwest. Its H I mass is $\sim 10^8 M_{\odot}$, a few percent of the total H I mass of the galaxy



Fig. 4-4

HI images of 34 galaxies observed in the THINGS program (Walter et al. 2008). All galaxies are shown on the same linear scale, indicated by the arrow in the lower right corner. For comparison, the HI disk of the Milky Way is displayed on the same scale in the center of the figure

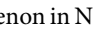
in the disk are a few $M_{\odot} \text{ pc}^{-2}$ in the inner parts, with local maxima of over $10 M_{\odot} \text{ pc}^{-2}$. Blitz and Rosolowsky (2006) investigated the effect of pressure in the ISM and suggested that above $10 M_{\odot} \text{ pc}^{-2}$ most of the hydrogen turns into molecular form. This is actually confirmed by observations (Bigiel et al. 2008).

HI disks exhibit a wealth of structure. This is very obvious in a bird's-eye view of 34 different galaxies from the THINGS survey (Fig. 4-4). In the inner parts, they exhibit the same structure as seen optically, traced by the recent star formation (spiral arms, spiral arm segments, filaments, etc.). The outer HI disks also exhibit structure, often with spiral arm-like features similar to the inner parts. Also in the outer disk, the brightest HI structures coincide often with locations of star formation as shown by the UV emission detected by GALEX in the outer disks of galaxies (Thilker et al. 2005, 2007). This is very clear in Figs. 4-1 and 4-9.

When examined globally, many galaxies exhibit asymmetries, both kinematically and spatially. Sancisi et al. (2008) examined some 300 galaxies in the WHISP sample and concluded that half of the objects are asymmetric. A more quantitative analysis by van Eymeren et al. (2011a, b) shows that more than 60% of the WHISP galaxies show kinematic and/or morphological asymmetries. The latter studies show that kinematic lopsidedness is more common than the occurrence of morphological asymmetries. The cause for asymmetries is not well established. Sancisi et al. (2008) suggest that accretion or minor mergers are the main cause. This could be fallback of material in tidally interacting systems, though not in every case as not all

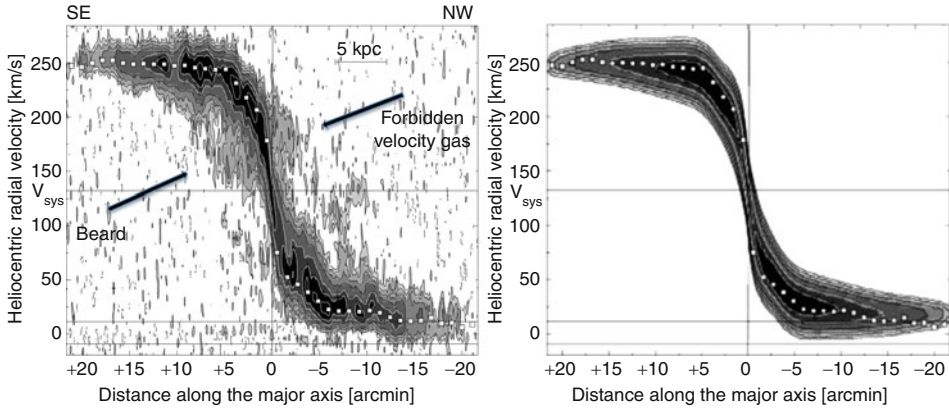
lopsided galaxies are interacting systems. van Eymeren et al. (2011b) investigate the dependence of the degree of lopsidedness on the environment and confirm that there is no clear effect. So if tidal interactions are the only way to induce lopsidedness, it needs to be long-lived.

In addition to global asymmetries, a large fraction of HI disks of galaxies appear warped (García-Ruiz et al. 2002; Sancisi et al. 2008). Warped HI disks are best studied in edge-on galaxies but can also be found and quantified through their signature in the HI velocity fields as described by Briggs (1990) and more recently by Józsa (2007) and Józsa et al. (2007). The warps usually start at the edge of the optical disk (García-Ruiz et al. 2002). As with the asymmetries in general, warps need to be long-lived if tidal interactions are the only cause, suggesting other mechanisms such as accretion and minor mergers (Sancisi et al. 2008). The warped HI layer of the Milky Way increases in thickness toward the outer parts (Levine et al. 2006; Kalberla and Kerp 2009). This thickening has not been established as well for other galaxies. Some well-studied edge-on galaxies have been shown to exhibit flaring HI layers (Sancisi and Allen 1979; Olling 1996; O'Brien et al. 2010), indicating that flaring HI disks may be very common. Further investigations combining accurate measurement of both the velocity dispersion of the gas and the thickness of the HI layer are required to confirm this trend for a larger number of galaxies. For a more detailed overview of the methods and results see Kregel and van der Kruit (2005 and references therein), O'Brien et al. (2010), and the review by van der Kruit and Freeman (2011). There is an indication that low-luminosity dwarf galaxies have thicker HI disks than normally found in spiral galaxies (Roychowdhury et al. 2009, 2010).

Detailed studies at increasing sensitivity and resolution of the nearby edge-on galaxy NGC 891 (Sancisi and Allen 1979; Swaters et al. 1997; Oosterloo et al. 2007a) have shown that there exist a thick HI disk and an HI halo. They are corotating with the disk, though the rotation slows down with increasing height above the plane. This decrease is too large (20–40 km s⁻¹) to be explained by asymmetric drift. The existence of a thick disk/halo can also be detected in moderately inclined galaxies as it becomes manifest by its slower rotation as gas at lower velocities in position-velocity diagrams (termed the “beard” by Schaap et al. 2000, who first identified and studied this component in NGC 2403). Fraternali et al. (2001, 2002) made a detailed study of this phenomenon in NGC 2403 using more sensitive HI data.  Figure 4-5 shows this “beard” in NGC 2403. Modeling showed that also in this galaxy the thick disk is rotating more slowly by a few tens of km s⁻¹ as is the case for NGC 891.

The indication for the possible existence of an extended gaseous halo around galaxies originally came from the detection of galactic absorption lines in the direction of bright stars in the Magellanic Clouds that could be ascribed to hot gas in a galactic “corona” (Savage and de Boer 1979). This component, often termed the warm ionized medium (WIM) or the diffuse ionized gas (DIG), has also been shown to be present in the disks and halos of other galaxies (Dettmar 1990; Rand et al. 1990). This thick WIM component in galaxies is thought to be fed by stellar winds and supernova explosions, though the number of “chimney”-like structures expected based on models such as those of Norman and Ikeuchi (1989) has not yet been confirmed by H_α imaging of edge-on galaxies. This phenomenon is also supposed to drive the outflow of neutral gas and be at the root of the “Galactic Fountain” mechanism (Bregman 1980; Kahn 1994; Rosen and Bregman 1995) in the disk-halo interface.

A related phenomenon discovered along with the thick HI disk and HI halo is the presence of gas complexes outside the thin HI disk. These were noted as either gas moving at velocities different from the general rotation in face-on galaxies (M 101: van der Hulst and Sancisi 1988; NGC 6946: Kamphuis and Sancisi 1993; Boomsma et al. 2008) or as features above the disk in edge-on galaxies (NGC 891: Oosterloo et al. 2007a). This anomalous-velocity gas appears to be



■ Fig. 4-5

Illustration of the “beard” phenomenon in the galaxy NGC 2403. The *left panel* shows a position-velocity cut along the major axis of NGC 2403 (adopted from Fraternali et al. 2001). Contours are $-0.4, 0.4, 1, 2, 4, 10, 20,$ and 40 mJy beam^{-1} . The *white symbols* represent the projected rotation curve, overplotted on the HI data. The *right panel* shows a model position-velocity diagram for a thin HI disk for comparison. The HI at anomalous velocities is marked by the *arrows* in the *left panel*. The two components are the “beard,” moving at velocities slower than the local rotation, and occasional HI structures moving at forbidden velocities

a mix of gas removed from the disk by a “Galactic Fountain” mechanism, related to massive star formation processes in the disk, and steady accretion of intergalactic gas or tidal debris, much like the mechanisms proposed for the presence of the high velocity clouds and the Magellanic Stream around the Milky Way (for more details see the review by Sancisi et al. 2008). The amount of HI in these features typically is of the order of $\sim 10^8 M_{\odot}$ or less than 10% of the total amount of HI in a typical disk galaxy.

The discovery of these features required long integrations (~ 100 h on current synthesis telescopes) and they have thus far been found only in a small number of galaxies. Large surveys of galaxies such as WHISP (van der Hulst et al. 2001) and THINGS (Walter et al. 2008) do not reach the required HI column density sensitivity well below 10^{20} cm^{-2} . A recent deep survey of ~ 20 galaxies (HALOGAS, Heald et al. 2011) is expected to provide more insight in these phenomena.

Detailed studies of HI in galaxies have been expanded to early-type galaxies (ETGs, usually S0s and ellipticals), systems which have less copious amounts of HI relative to their stellar or total mass. The picture that emerges here (Oosterloo et al. 2007b, c, 2010a; Serra et al. 2012) is that roughly half of the ETGs in the field are detected in HI with detection limits of a few times $10^6 M_{\odot}$. About half of these exhibit large, regularly rotating HI disks or rings, while many objects show the presence of tails and outlying HI structures reminiscent of tidal effects and accretion.

In dense environments such as the Virgo cluster, the HI properties of galaxies change drastically as a result of tidal interactions and interaction with the intracluster medium (e.g., see Chung et al. 2009; Solanes et al. 2001). In Virgo, only 10% of the ETGs are detected (Serra et al. 2012), while the spiral galaxies show truncated HI disks and clear signs of stripping and interactions (Chung et al. 2009). These effects will be discussed in more detail in [Sect. 4](#).

At the other extreme, there are the low-luminosity and low-surface-brightness galaxies in the field. Some 65 small, low-luminosity ($M_B > -15$) dwarf irregular galaxies have been studied recently with the GMRT (the Faint Irregular Galaxies GMRT Survey (FIGGS), Begum et al. 2005, 2008) and confirm existing trends in that the HI to optical sizes of galaxies increases toward lower optical luminosities (implying also an increase in M_{HI}/L_B with decreasing luminosity). These low-luminosity systems continue to obey the $M_{\text{HI}}/D_{\text{HI}}$ relation first demonstrated by Broeils and Rhee (1997), indicating that the average HI surface densities are similar to those in the HI disks of more luminous galaxies. Complementary surveys, carried out with the VLA and focusing on studies of the HI in nearby, low-mass star-forming galaxies, are LITTLE-THINGS (Hunter et al. 2011) and VLA/ANGST (Ott et al. 2008).

The classical low-surface-brightness galaxies (van der Hulst et al. 1993; de Blok et al. 1996) appear to fill the gap between these very-low-luminosity systems and the galaxies of normal surface brightness and normal luminosity in terms of their properties.

2.3 The Warm and Cold ISM in Galaxies

The presence of ionized hydrogen around OB stars, in the form of H II regions, has been known for a long time. The idea that in addition the ISM in the Galaxy may have a more widespread, hot, ionized hydrogen component came from the interpretation of the low-frequency turnover of the spectrum of the Galactic synchrotron emission as free-free absorption (Hoyle and Ellis 1963). Ten years later, the presence of the diffuse ionized interstellar medium was clearly demonstrated from the detection of ubiquitous H α emission (Reynolds 1971; Reynolds et al. 1973). Another 20 years later, Dettmar (1990) and Rand et al. (1990) showed with deep H α imaging of NGC891 that other galaxies also have such a warm, ionized component. A very complete and recent review of this so-called warm ionized medium (WIM) in galaxies has been given by Haffner et al. (2009).

The presence of dust in the ISM has been obvious for centuries: naked-eye observations of the central Milky Way show large dark patches of obscured starlight, bearing witness to the presence of obscuring material. Similar structures are also evident from images of other galaxies, where dust features outline the sometimes regular, sometimes chaotic spiral structure in galaxy disks. A major leap in studying dust in galaxies has come from infrared astronomy as noted in an early review (Stein and Soifer 1983) written at the dawn of routine mid-IR and far-IR imaging. A major breakthrough came from imaging of galaxies in the far-IR by IRAS (<http://irsa.ipac.caltech.edu/IRASdocs/iras.html>), and later the Infrared Space Observatory (ISO; <http://iso.esac.esa.int>), SPITZER (<http://www.spitzer.caltech.edu>), and HERSCHEL (<http://www.esa.int/herschel>). Not only detailed spectral energy distributions are now available, supporting the models describing the overall IR spectrum as thermal emission from cold dust, but also many spectral features resulting from complex molecules, primarily Polycyclic Aromatic Hydrocarbons (PAHs; see ► Chap. 10 of Volume 5) providing better insight in the interpretation of mid-IR and far-IR images of galaxies.

The tradition of observing HI and H II in galaxies is by now half a century old. The realization that molecules in the ISM can also be imaged using radio lines came almost two decades later with the first detection of CO in the Galaxy in 1970 (Wilson et al. 1970) and the first extragalactic CO detection in M 82 and NGC 253 in 1975 (Rickard et al. 1975a, b). The CO emission indirectly traces H₂, as rotational transitions of the CO molecules are excited by collisions with hydrogen molecules. Unfortunately, it is very difficult to observe the cold H₂ directly. Electronic

transitions are very faint and occur in the ultraviolet where both the Earth's atmosphere and interstellar extinction obstruct our view (Shull and Beckwith 1982; Habart et al. 2005). Rotational transitions occur in the mid-infrared (Black and van Dishoeck 1987) at 28.2, 17.0, and 12.3 μm . H_2 can also be observed at shorter wavelengths when the temperature increases to several hundred K, but this only occurs around hot stars and active galactic nuclei (AGN). These lines of cold molecular hydrogen are weak and require very high column densities to be observable. So far, only detections of fairly warm gas have been made in the edge-on disk of NGC 891 (Valentijn and van der Werf 1999) and the nucleus of NGC 6946 (Valentijn et al. 1996).

Young and Scoville (1991) reviewed the early work on the CO and hence molecular content of galaxies, mostly carried out with single-dish radio telescopes. The first detailed images came with the advent of mm arrays and eventually large observing programs such as BIMA-SONG (Regan et al. 2001; Helfer et al. 2003) and HERACLES (Leroy et al. 2008, 2009).

A major uncertainty remains the conversion from CO brightness to H_2 column density. The general relation is expressed as

$$\frac{N_{\text{H}_2}}{\text{cm}^{-2}} = X_{\text{CO}} \int \frac{I_{\text{CO}}(\nu)}{\text{K kms}^{-1}} d\nu \quad (4.7)$$

The commonly adopted value for X_{CO} is the value determined for Galactic molecular clouds, $X_{\text{CO}} = 3 \times 10^{20} \text{ cm}^{-2} (\text{K km s}^{-1})^{-1}$. This conversion factor has, however, been demonstrated to depend on metallicity and can be uncertain by an order of magnitude (Wilson 1995; Israel 1997; Leroy et al. 2011a; see also Shetty et al. 2011a, b; Liszt et al. 2010 for a theoretical treatment of the X_{CO} conversion factor for both dense and diffuse molecular gas).

3 Star Formation and the ISM


The transformation of gas into stars is one of the most important processes in galaxy evolution. Understanding the conditions that determine the efficiency of this process, and the associated physics, is the goal of many observational and theoretical studies. They also form important input into numerical computer models of galaxy formation and evolution. A complete understanding requires knowledge of these processes over a large range in scales: from galaxy-sized scales where gas is transported from the disk of the galaxy into the halo and back (which is also the scale where accretion and capture of satellites takes place) to kpc-sized scales where gas clouds are coalescing, via sub-kpc scales where neutral gas cools and forms molecular gas in GMCs, to parsec scales where individual stars are formed.

These very small scales can be directly observed in our Galaxy, while the processes happening at galaxy scales can in principle be studied in external galaxies. Tying together the processes happening at these two extreme scales has been a major challenge in this particular field: in our Galaxy, we lack the overview we have for other galaxies, while we rarely have the resolution to study the detailed processes leading to star formation in external galaxies.

This led to many studies exploring empirical relations between the properties (usually surface or volume density) of the gas component and some kind of tracer of the recent star formation. In the last couple of years, significant progress has been made with the advent of high-resolution multiwavelength surveys of the gas and star formation components. These surveys are now starting to bridge the gap between the observations at the scales of stars and those at scales of galaxies.

Schmidt (1959) was the first to relate the gas density in our Galaxy to the star formation rate (SFR) using a relation $\rho_{\text{SFR}} \sim \rho_{\text{gas}}^n$. He found a value $n \simeq 2$. Schmidt's relation between volume densities can be translated into a relation involving surface densities $\Sigma_{\text{SFR}} \sim \Sigma_{\text{gas}}^N$. Surface densities are more easily quantifiable in external galaxies, and the exponents n and N are related as long as the scale height of the disk is constant. This kind of relation has become known as the "Schmidt Law," and the name is commonly used for any sort of relation that describes the link between a gas component (neutral, molecular, or global) and a star formation tracer (young stars, ionized gas emission, infrared emission).

The first investigations of the Schmidt Law in external galaxies were done by Sanduleak (1969) and Hartwick (1971), who looked at young stars and star-forming regions in the SMC and M31. Madore et al. (1974), Newton (1980), Tosa and Hamajima (1975), and Hamajima and Tosa (1975) followed up on this by studying the relation between young stars and HI surface density in nearby galaxies such as M31, the LMC, M101 and others. These studies found $N \simeq 2$ but with a large spread of a few tens of percent.

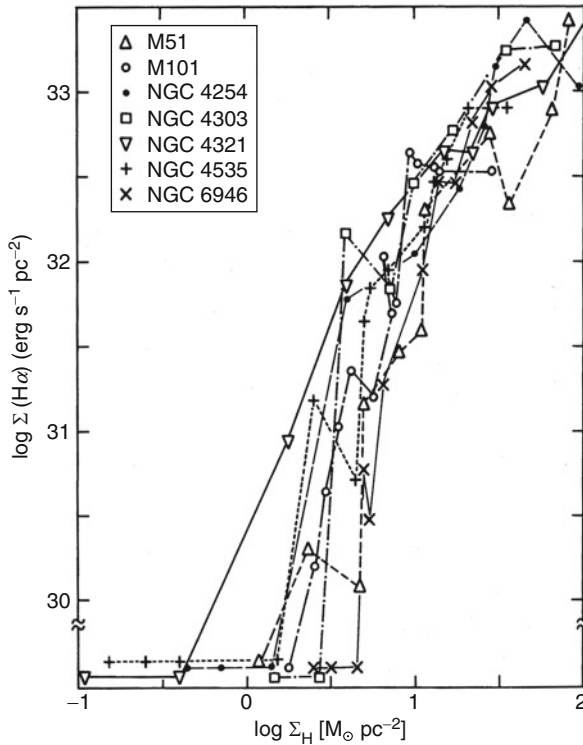
In a landmark paper, Kennicutt (1989) (see also Kennicutt 1998) studied the averaged gas and H α content of 61 nearby spirals and 36 starburst galaxies. He derived a Schmidt Law between the total gas surface density $\Sigma_{\text{gas}} = \Sigma_{\text{HI}} + \Sigma_{\text{H}_2}$ and the H α -derived SFR with values of $N = 2.47 \pm 0.39$ for spirals and $N = 1.40 \pm 0.15$ for all galaxies (spirals and starbursts) in his sample. As a result of this work, the relation between gas surface density and star formation is often referred to as the "Kennicutt-Schmidt Law."  Figure 4-6 shows this result as presented in the Kennicutt (1989) paper.

Similar studies, using different measures for the gas surface density, and different star formation tracers (such as ultraviolet or infrared emission) found similar values, but again with a large spread. This may reflect actual variations in the physics, but a large part of this spread is very likely also due to choice of sample, analysis, and star formation tracers. For a description of these studies, see the review by Kennicutt (1998).

Kennicutt (1989, 1998) and Martin and Kennicutt (2001) also found evidence for a star formation threshold. That is, the star formation efficiency (as traced by H α) decreases dramatically once the gas surface density drops below a certain threshold, but star formation does not shut off completely (e.g., Ferguson et al. 1998). Kennicutt (1989) relates this star formation threshold density to the Toomre Q parameter and the stability of the disk.

A similar cutoff behavior in the star formation efficiency had also been observed by Skillman (1987), who noted that star formation (again, as traced by H α) did not seem to occur below a (constant) H I surface density threshold of $\sim 1 \cdot 10^{21} \text{ cm}^{-2}$. The star formation threshold was also suggested by van der Hulst et al. (1993) as an explanation for the low star formation rates observed in low surface brightness (LSB) galaxies. These galaxies generally have lower H I surface densities than "normal" galaxies (de Blok et al. 1996). Though this is not the place to review the large body of theoretical and numerical work on the relation between gas (surface) density and star formation rate, we note the work by Schaye (2004) and Taylor and Webster (2005) who suggest that the star formation threshold is related to the formation of a cold phase in the neutral ISM when a sufficiently high surface density is reached. This cold phase makes efficient cooling suddenly possible, leading to star formation.

Over the last decade, the amount of high-resolution, multiwavelength information about galaxies in the nearby universe has increased dramatically. This had made possible new studies of the conditions for star formation on kpc or even sub-kpc scales in a significant number of galaxies. Here we summarize some of the main results derived and refer to these papers for further references.

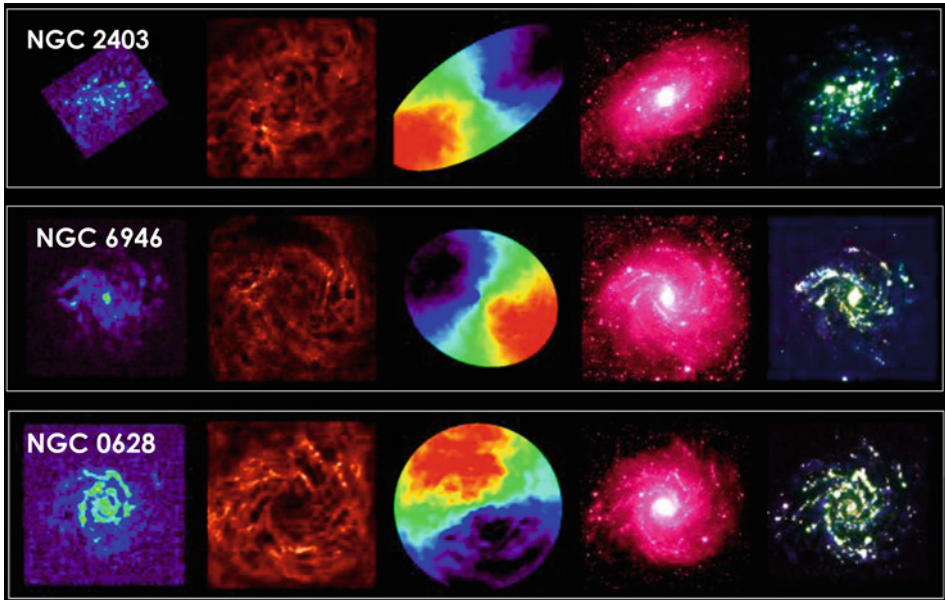


■ Fig. 4-6

Star formation surface density (measured from the $H\alpha$ emission) as a function of gas surface density (measured from HI and H_2 (i.e., CO) observations) in seven well-resolved, nearby galaxies (Adopted from Kennicutt 1989)

Bigiel et al. (2008) investigated relations of the star formation rate surface density Σ_{SFR} with the HI surface density Σ_{HI} , the molecular surface density Σ_{H_2} and the combined gas surface density Σ_{gas} on scales of 750 pc in a number of nearby disk and dwarf galaxies. The star-formation rate maps were based on a combination of GALEX FUV maps and Spitzer 24 μm maps from respectively the GALEX NGS (Gil de Paz et al. 2007) and the Spitzer Infrared Nearby Galaxies Survey (SINGS; Kennicutt et al. 2003). For the gas surface densities, information was used from THINGS (Walter et al. 2008) for the neutral part of the ISM, and HERACLES (Leroy et al. 2009) and BIMA-SONG (Helfer et al. 2003) for the molecular part (as traced by the CO line). ● Figure 4-7 shows three galaxies with such detailed information: the distribution of molecular hydrogen, atomic hydrogen, the kinematics of the atomic hydrogen, the distribution of near-IR light (predominantly old stars), and a composite of UV light, mid-IR light, and $H\alpha$ emission (tracing star formation).

It was found that, at least in the star-forming disks of the sample galaxies, a strong relation exists between Σ_{H_2} and Σ_{SFR} , with a power-law exponent $N = 1.0 \pm 0.2$, i.e., a linear relation. This can be interpreted as stars forming from the molecular ISM at a constant efficiency. This agrees with a result from Kennicutt (1989) who had found a similar relation for starburst galaxies,



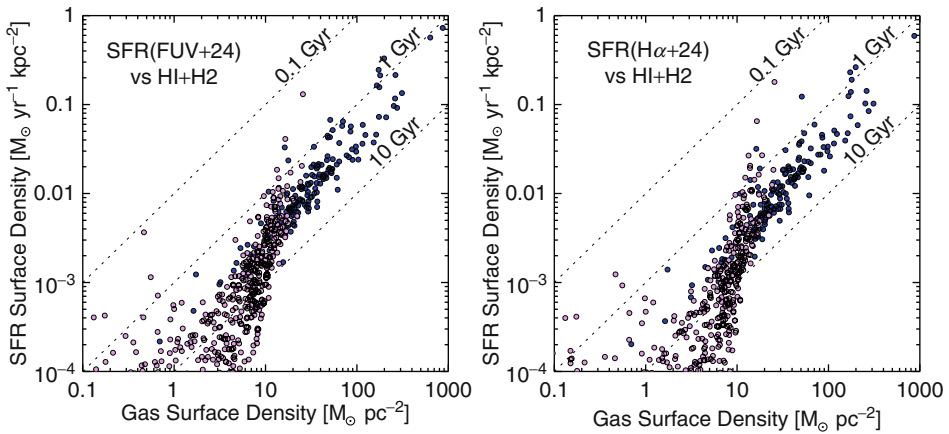
■ Fig. 4-7

Three examples of the wealth of information available to study the relation between gas density, gas kinematics, and star formation in detail (courtesy Adam Leroy and the HERACLES team, Leroy et al. 2012, 2011b). From left to right: distribution of CO (as proxy for H₂) (HERACLES), distribution of HI (THINGS), HI velocity field, near-IR image (SPITZER: SINGS and LVL), and composite image from GALEX FUV, SINGS/LVL mid-IR, and SINGS/LVL H α emission showing the distribution of star formation

where the H₂ surface densities are much higher. This is illustrated in ► Fig. 4-8 (adopted from Fig. 10 of Schruba et al. 2011), which shows two different measures of the star formation surface density versus the gas surface density. The power-law regime applies to gas surface densities above $10 M_{\odot} \text{pc}^{-2}$.

Note, though, that the Bigiel et al. (2008) result does not say anything about the necessary conditions for star formation inside GMCs. At the working resolution of 750 pc, GMCs are not resolved, and the linear relation found must therefore be interpreted within the context of “counting clouds,” i.e., they can be explained by assuming that the GMCs have uniform properties with the observed CO surface density determined by the beam filling factor of these clouds.

Bigiel et al. (2008) found less well-defined relations between Σ_{gas} or Σ_{HI} on the one hand and Σ_{SFR} on the other hand. The relation between Σ_{gas} and Σ_{SFR} was found to vary from galaxy to galaxy, and there is almost no relation with Σ_{HI} . These results were revisited by Schruba et al. (2011) who used stacking of the HERACLES CO data (using HI radial velocities as a prior) to push the CO detections to larger radii. In these outer parts, the gas content is dominated by the neutral HI rather than the molecular H₂. In this lower gas surface density regime, the star formation law changes its linear behavior. This is clear in ► Fig. 4-8.

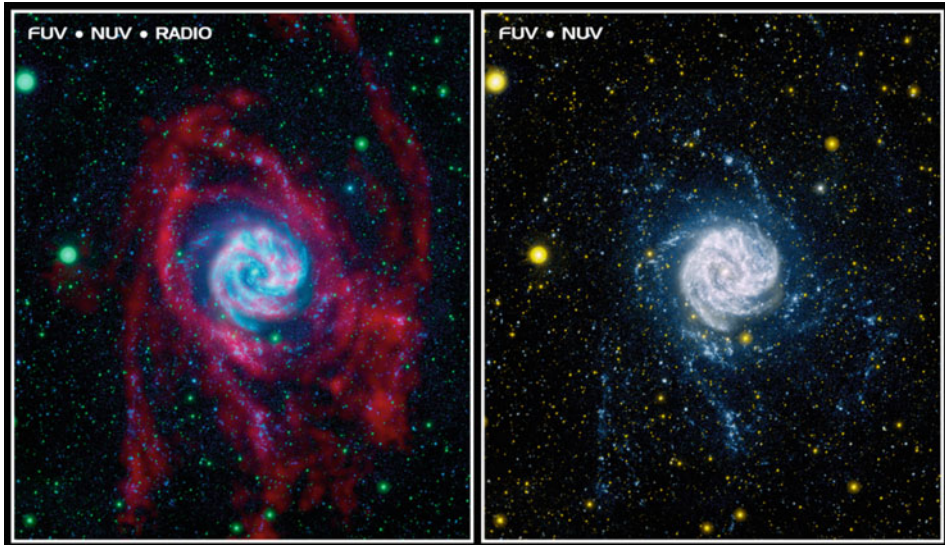


■ Fig. 4-8

Σ_{SFR} (y-axis) from FUV + $24 \mu\text{m}$ (left) and $H\alpha$ + $24 \mu\text{m}$ (right) as a function of gas surface density ($H I + H_2$). Each point represents a radial average in a given galaxy. Regions that are H_2 dominated are plotted with dark blue symbols, regions that are $H I$ dominated in light red symbols. Whereas SFR is not correlated with $H I$ (in the inner parts of galaxy disks), it correlates with H_2 and total gas surface density. The scaling exhibits a change in slope at the transition between $H I$ - and H_2 -dominated environments (This figure is adopted from Fig. 11 in Schruha et al. 2011)

Schruha et al. (2011) found that the linear relation between Σ_{H_2} and Σ_{SFR} extends into this $H I$ -dominated regime. One interpretation of these results is that the Kennicutt-Schmidt Law can be separated into two separate processes. The first one is star formation proceeding with a constant efficiency once H_2 is formed. The “bottleneck” determining the star formation rate thus seems to be the second process of conversion from $H I$ into H_2 (likely through the formation of a cold neutral component as discussed earlier). The star-formation threshold as found by Kennicutt (1989) therefore seems to be caused by a change in SFR due to a changing ratio of $H I$ to H_2 (as a function of total gas density) rather than an actual shutting off of star formation.

This is supported by the realization that star formation in the outer parts of disks is more widespread than originally thought. The early observations of Ferguson et al. (1998) showed isolated star-forming regions (as traced by $H\alpha$) well beyond the optical disks of a number of nearby galaxies. The discovery of further star formation using GALEX observations in the UV showed that these early observations were showing only the tip of the iceberg (Thilker et al. 2005). The UV observations enabled direct detection of O and B stars which would otherwise have escaped detection due to their inability to excite the surrounding ISM enough to produce $H\alpha$ emission. It is now thought that these so-called extended UV (XUV) disks are found in $\sim 30\%$ of nearby disk galaxies (Thilker et al. 2007). A striking example is M 83 (NGC 5236) shown in [Fig. 4-9](#): the outlying $H I$ structures show up remarkably well in the UV, indicating that star formation is progressing there as well, albeit with a lower efficiency (Bigiel et al. 2010b) than in the bright, inner region of the galaxy. A comparison of star formation as traced by $H\alpha$ with star formation as traced by UV radiation from O and B stars shows that while the level of $H\alpha$ emission typically drops very steeply at the edge of the optical disk (giving the appearance of a star formation threshold), such an edge is not observed in the UV emission. Rather, the



■ Fig. 4-9

THINGS HI image (Walter et al. 2008) superposed on a near- and far-UV composite image (Thilker et al. 2005; Bigiel et al. 2010a) of M 83 (*left panel*). For better comparison of the faint outer star formation structures the single UV composite image is shown as well (*right panel*). Note the extended structures, (arms, arcs, filaments) in the outer disk, visible in both the HI and the UV images, indicating that even in the faint outer HI star formation is progressing (Courtesy Dave Thilker and NASA/JPL-Caltech/VLA/MPIA)

density of young stars gradually decreases, again supporting the idea that the changing ratio of HI to H₂ ultimately determines the overall star formation efficiency.

The above broad-brush picture illustrates the progress made in the last few years, and these results can now be used as input for numerical models that can help explain variations of star formation efficiency with, e.g., redshift, environment, or galaxy mass.

It is, however, still difficult to link the observations with the actual physical processes driving the star formation rate. Leroy et al. (2008) used the same data set as Bigiel et al. (2008) to test a number of theoretical explanations proposed in the literature linking the gas density and the SFR. They looked at the disk free-fall time, the orbital timescale, the effects of cloud-cloud collisions, the assumption of fixed GMC star formation efficiency, and the relation between pressure in the ISM and the phases of the ISM.


Similarly, they investigated several models proposed for the star formation threshold, such as gravitational stability in a gas disk, gravitational stability in a mixed disk of gas and stars, the effects of shear in a disk, and the onset of a cold gas phase.

Their conclusions were that none of these offers a unique explanation for the observed behavior. While large-scale relations can be identified (such as the Kennicutt-Schmidt Law), the actual physics remains more complicated, and still below the resolutions achieved so far. Observationally we will also have to get a better understanding of the balance between warm and cold HI phases, the efficiency of H₂ formation, and possibly the effects of shocks and turbulence. Many of these have already been studied numerically or theoretically. In the next decade or so we, should be able to obtain the observational evidence in a large number of galaxies at


sufficient resolution in order to gauge the ability of the ISM to form GMCs over a wide range of galaxy conditions.

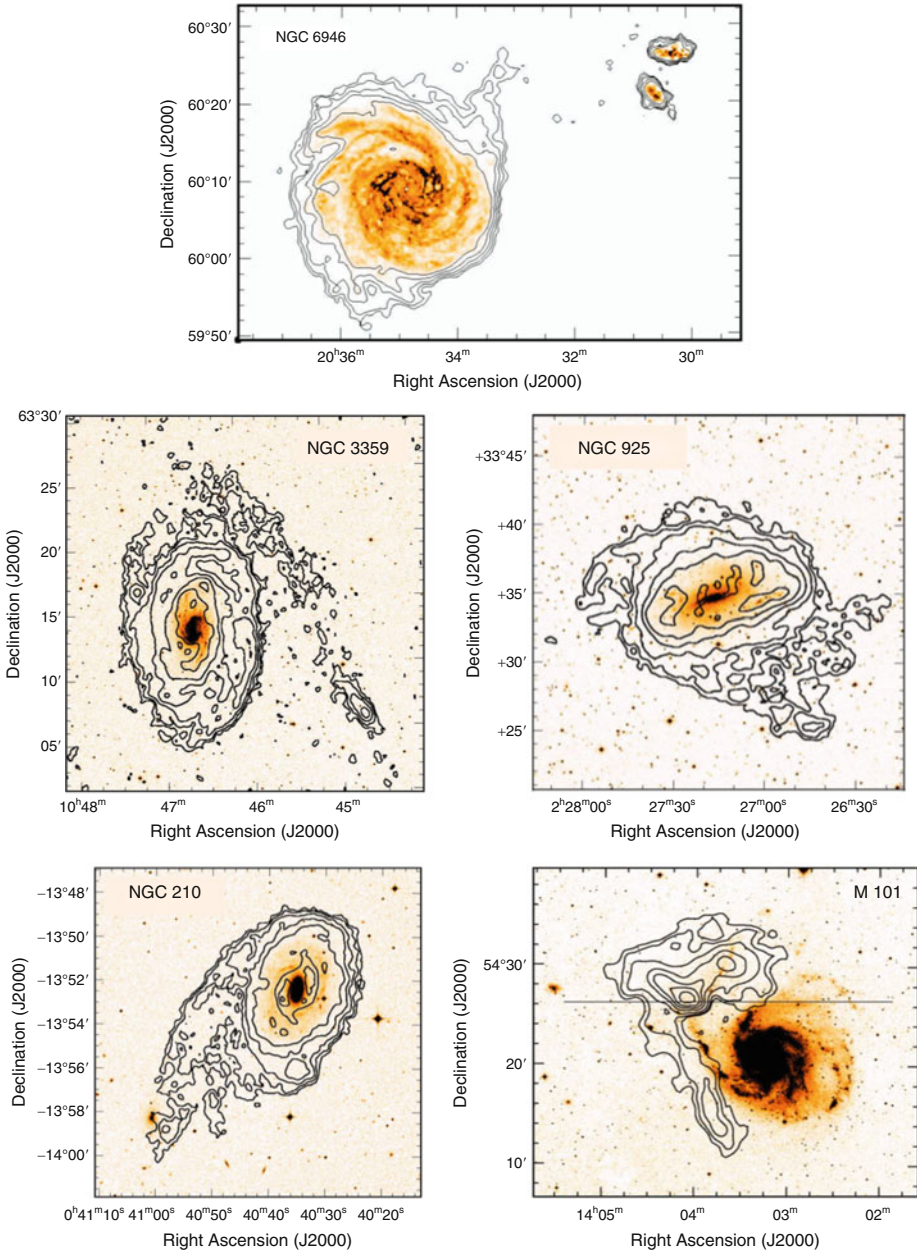
4 Accretion, Feedback and the Environment

One of the main puzzles in galaxy evolution is that the rate at which new stars have formed in galaxies has declined dramatically over the last 7 Gyr (e.g., Madau et al. 1998; Hopkins and Beacom 2006), in contrast to the lack of a similar decline in the estimated cold gas density in the universe (Lah et al. 2007). Observed star formation rates in galaxies are such that the observed gas supply is exhausted in a few Gyr (e.g., Bigiel et al. 2008) and the dwindling star formation could, in principle, be due to star formation consuming the available gas supply. Galaxies must, therefore, continuously accrete gas from the intergalactic environment to keep the observed gas density levels. Continuous accretion of gas from the IGM may solve this discrepancy so that star formation can continue over much longer periods than given by the initial gas reservoirs and the gas consumption times.

The observational evidence for accretion has been extensively described in the review of Sancisi et al. (2008), who examine a number of H I signatures in galaxies in the nearby universe. Examples are small (and often subtle) asymmetries in the distribution and/or kinematics of the H I (lopsidedness), the presence of warps, of small H I companions, faint H I tails and other structures, and the presence of extraplanar gas (a prime example being NGC 891, Oosterloo et al. (2007a)).  Figure 4-10 provides a few examples of galaxies with this kind of evidence for accretion. From an inventory of such H I signatures in WHISP (van der Hulst et al. 2001; Sancisi et al. 2008) estimate an accretion rate of $\sim 0.2 M_{\odot} \text{year}^{-1}$ in H I. This number is very uncertain and does not account for the accretion of warm, ionized gas.

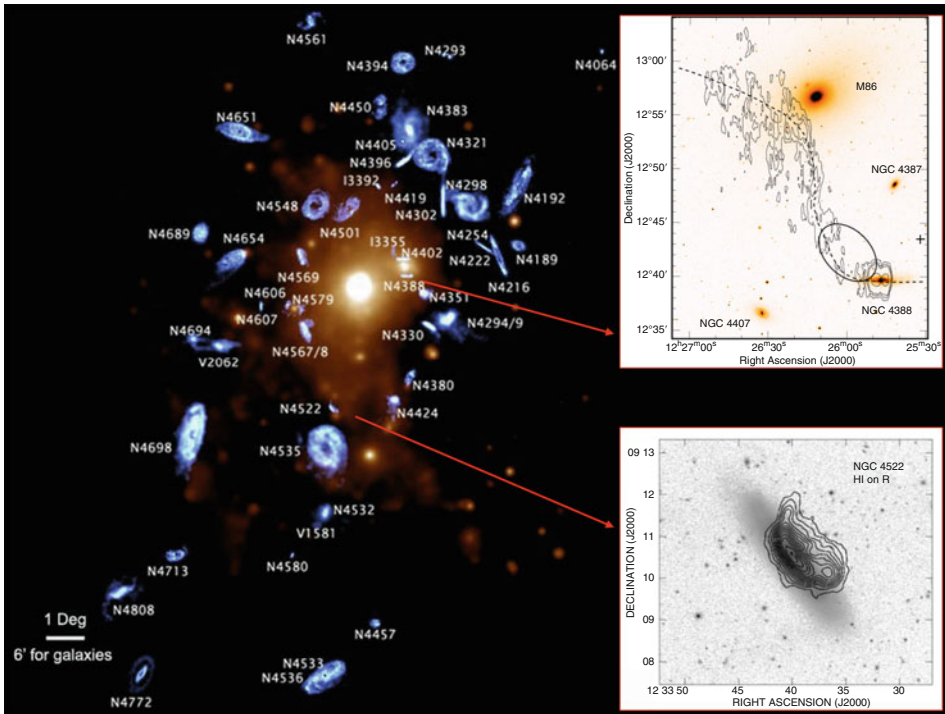
From the theoretical point of view, there is increasing evidence that so-called cold-mode accretion plays an important role in providing the dark matter halos with the fuel for forming stars and building up the stellar mass in galaxies (Birnboim and Dekel 2003; Dekel and Birnboim 2006; Binney 2004; Kereš et al. 2005; Cattaneo et al. 2006; Kereš et al. 2009a). Cosmological simulations suggest that cold-mode accretion is the dominant process at redshifts $z \geq 2$ but becomes less important at lower redshifts (van de Voort et al. 2011). The cold-mode accretion has been examined closely in the Milky Way and a few nearby galaxies (NGC 891 and NGC 2403) by Fraternali and Binney (2008), Marinacci et al. (2010) and Binney and Fraternali (2012), in particular with the goal of verifying theoretically what fraction of the gas in the halo of the Milky Way results from accretion versus gas brought into the halo by the “Galactic Fountain” mechanism. Marasco and Fraternali (2011) and Marasco et al. (2012) conclude from detailed modeling of the halo of the Milky Way that the “Galactic Fountain” induces a steady inflow of $\sim 2 M_{\odot} \text{year}^{-1}$, enough to sustain the star formation in the disk and an order of magnitude larger than the accretion rate estimated by Sancisi et al. (2008).

Accretion is not the only process relevant to the interplay between star formation and the environment. Gas removal processes can be equally important depending on internal processes (stellar winds, supernovae, presence of an AGN) or external, environmental conditions (density of the intergalactic medium (IGM), local galaxy density, i.e., the probability of gravitational interactions). Examples of such external processes are plentiful in the denser environments of clusters and groups. The best observational evidence is found in the Virgo cluster ( Fig. 4-11), which offered the first clear effects of gas removal by ram pressure in the hot intracluster gas and gravitational interactions (Warmels 1988; Cayatte et al. 1994; Chung et al. 2009). These studies



■ Fig. 4-10

Five examples of HI structures which could be the result of recent interactions/accretion. In each panel, the contours show the HI density distribution superposed on the optical image. For NGC 6946, the column density levels are 1.25, 2.5, 5, and $20 \times 10^{19} \text{ cm}^{-2}$; for NGC 3359, 10, 20, 50, 100, 200, $400 \times 10^{19} \text{ cm}^{-2}$; for NGC 925, 5, 10, 20, 50, $100 \times 10^{19} \text{ cm}^{-2}$; for NGC 210, 5, 10, 20, 50, $100, 200 \times 10^{19} \text{ cm}^{-2}$; and for M 101, 0.7, 1.4, 2.8, 5.6, 8.4, 11.2, $14.0 \times 10^{19} \text{ cm}^{-2}$. In M101 only the high velocity gas is shown. (Images are courtesy of Oosterloo and Sancisi, and from Boomsma et al. 2008 and Kamphuis 1993)

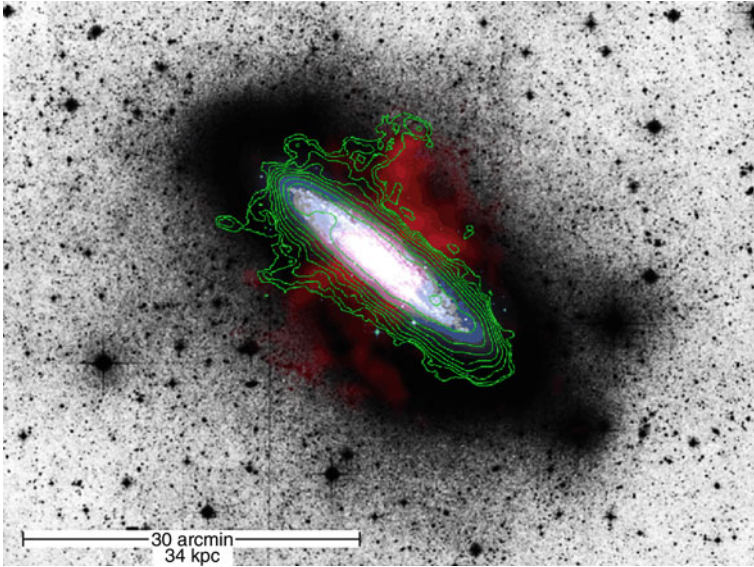


■ Fig. 4-11

Examples of effects of the environment in the Virgo cluster. The *right panel* shows the central part of the Virgo cluster with in red the X-ray emission from the intracluster gas and individual massive galaxies and in blue the H I distributions of the galaxies imaged with the VLA by Chung et al. (2009). Note that the H I disks are enlarged by a factor 10 for visible presentation. The H I disks in the core of the Virgo cluster are clearly smaller than those of galaxies in the outer parts. To the *right*, two particular examples of ram pressure stripping are enlarged: NGC 4388 (Oosterloo and van Gorkom 2005) and NGC 4522 (Kenney et al. 2004)

showed that all galaxies are systematically small in H I in the cluster core where the IGM density is highest (☉ Fig. 4-11), with two clear examples of ongoing ram pressure stripping: NGC 4522 (Kenney et al. 2004), and NGC 4388 (Oosterloo and van Gorkom 2005). These studies provided insight into why the relative H I content in galaxies in dense environments is low (Solanes et al. 2001).

Internal gas removal processes, often referred to as “feedback,” are most obvious in galaxies with either an AGN or a massive starburst. Very telling examples are the nearby galaxies M 82 and NGC 253. ☛ Figure 4-12 shows the H I, the ionized gas and the hot X-ray gas blown out of the central disk by the massive nuclear starburst in NGC 253 (Boomsma et al. 2005). For a review of such massive starbursts, see Heckman et al. (1993). These phenomena are much more energetic than the moderate “Galactic Fountain” mechanism but may have much shorter duration. The combination of such processes has been implemented in theoretical models describing galaxy evolution (Cook et al. 2010; Kereš et al. 2009a, b; Springel et al. 2005) and



■ Fig. 4-12

Deep optical image of NGC 253 with superposed HI column density contours (in green at 0.18, 0.36, 0.72, 1.4, 2.9, 5.8, 12, and $23 \times 10^{20} \text{ cm}^{-2}$) and 0.1–0.4 keV X-ray emission (in red). The nuclear outburst is clearly visible in X-rays outlining the hot gas, and in HI outlining the cooler gas at the periphery of the nuclear wind (Boomsma et al. 2005)

appears to be important for regulating the star formation such that the observed luminosity and HI mass functions can be reproduced.

Understanding the balance between gas removal and gas accretion processes, including the role of the environment, will be a crucial element of understanding galaxy evolution. Though the current work on HI in a variety of environments is beginning to provide insight (van Gorkom 2008, 2011), it is based on only a small number of cases. New facilities, recently or soon available, will image an order of magnitude more galaxies and therefore contribute significantly to determining this balance. Such facilities are ALMA, the E-VLA, APERTIF on the WSRT (Verheijen et al. 2008, 2009; Oosterloo et al. 2010b), MeerKAT (de Blok et al. 2010; de Blok 2011), and ASKAP (Johnston et al. 2009; Westmeier and Johnston 2010).

References

- Baldwin, J. E., Field, C., Warner, P. J., & Wright, M. C. H. 1971, MNRAS, 154, 445
- Battaglia, G., Fraternali, F., Oosterloo, T., & Sancisi, R. 2005, A&A, 447, 49
- Begum, A., Chengalur, J. N., & Karachentsev, I. D. 2005, A&A, 433, L1
- Begum, A., Chengalur, J. N., Karachentsev, I. D., Sharina, M. E., & Kaisin, S. S. 2008, MNRAS, 386, 1667 (FIGGS)
- Bigiel, F., Leroy, A., Walter, F., Brinks, E., de Blok, W. J. G., Madore, B., & Thornley, M. D. 2008, AJ, 136, 2846 (THINGS)
- Bigiel, F., Leroy, A., Seibert, M., Walter, F., Blitz, L., Thilker, D., & Madore, B. 2010, ApJ, 720, L31
- Bigiel, F., Leroy, A., Walter, F., Blitz, L., Brinks, E., de Blok, W. J. G., & Madore, B. 2010, AJ, 140, 1194
- Binney, J. 2004, MNRAS, 347, 1093
- Binney, J., & Fraternali, F. 2012, EPJWC, 19, 8001

- Birnboim, Y., & Dekel, A. 2003, *MNRAS*, 345, 349
- Black, J. H., & van Dishoeck, E. F. 1987, *ApJ*, 322, 412
- Blitz, L., & Rosolowsky, E. 2006, *ApJ*, 650, 933
- Boomsma, R., Oosterloo, T. A., Fraternali, F., van der Hulst, J. M., & Sancisi, R. 2005, *A&A*, 431, 65
- Boomsma, R., Oosterloo, T. A., Fraternali, F., van der Hulst, J. M., & Sancisi, R. 2008, *A&A*, 490, 555
- Bregman, J. N. 1980, *ApJ*, 236, 577
- Briggs, F. H. 1990, *ApJ*, 352, 15
- Broeils, A. H., & Rhee, M.-H. 1997, *A&A*, 324, 877
- Cattaneo, A., Dekel, A., Devriendt, J., Guiderdoni, B., & Blaizot, J. 2006, *MNRAS*, 370, 1651
- Cayatte, V., Kotanyi, C., Balkowski, C., & van Gorkom, J. H. 1994, *AJ*, 107, 1003
- Chung, A., van Gorkom, J. H., Kenney, J. D. P., Crowl, H., & Vollmer, B. 2009, *AJ*, 138, 1741
- Cook, M., Barausse, E., Evoli, C., Lapi, A., & Granato, G. L. 2010, *MNRAS*, 402, 2113
- de Blok, W. J. G., McGaugh, S. S., & van der Hulst, J. M. 1996, *MNRAS*, 283, 18
- de Blok, W. J. G. 2011, *IAU Symp.*, 277, 96
- de Blok, E. W. J. G., Booth, R., Jonas, J., & Fanaroff, B. 2010, *PoS (ISKAF2010) 005*, http://pos.sissa.it/archive/conferences/112/005/ISKAF2010_005.pdf
- Dekel, A., & Birnboim, Y. 2006, *MNRAS*, 368, 2
- Dettmar, R.-J. 1990, *A&A*, 232, L15
- Ewen, H. I., & Purcell, E. M. 1951, *Nature*, 168, 356
- Ferguson, A. M. N., Wyse, R. F. G., Gallagher, J. S., & Hunter, D. A. 1998, *ApJ*, 506, 19L
- Field, G. B. 1959, *ApJ*, 129, 536
- Fraternali, F., Oosterloo, T., Sancisi, R., & van Moorsel, G. 2001, *ApJ*, 562, 47
- Fraternali, F., van Moorsel, G., Sancisi, R., & Oosterloo, T. 2002, *AJ*, 123, 3124
- Fraternali, F., & Binney, J. J. 2008, *MNRAS*, 386, 935
- García-Ruiz, I., Sancisi, R., & Kuijken, K. 2002, *A&A*, 394, 769 (WHISP)
- Gil de Paz, A., et al. 2007, *ApJS*, 173, 185
- Giovanelli, R., et al. 2005, *AJ*, 130, 2598 and 2613 (ALFALFA)
- Habart, E., Walmsley, M., Verstraete, L., Cazaux, S., Maiolino, R., Cox, P., Boulanger, F., & Pineau des Forêts, G. 2005, *Space Sci. Rev.*, 119, 71
- Haffner, L. M., Dettmar, R.-J., Beckman, J. E., et al. 2009, *Rev. Mod. Phys.*, 81, 969
- Hamajima, K., & Tosa, M. 1975, *PASJ*, 27, 561
- Hartwick, F. D. A. 1971, *ApJ*, 163, 431
- Heald, G., et al. 2011, *A&A*, 526, A118 (HALOGAS)
- Heckman, T. M., Lehnert, M. D., & Armus, L. 1993, *The environment and evolution of galaxies. Astrophys. Space Sci. Libr.*, 188, 455
- Helper, T. T., Thornley, M. D., Regan, M. W., Wong, T., Sheth, K., Vogel, S. N., Blitz, L., & Bock, D. C.-J. 2003, *ApJS*, 145, 259 (BIMA-SONG)
- Hopkins, A. M., & Beacom, J. F. 2006, *ApJ*, 651, 142
- Hoyle, F., & Ellis, G. R. A. 1963, *Aust. J. Phys.*, 16, 1
- Hunter, D. A., Elmegreen, B. G., Oh, S.-H., et al. 2011, *AJ*, 142, 121 (LITTLE-THINGS)
- Israel, F. P. 1997, *A&A*, 328, 471
- Johnston, S., Feain, I. J., & Gupta, N. 2009, *ASPC*, 407, 446
- Józsa, G. I. G., Kenn, F., Klein, U., & Oosterloo, T. A. 2007, *A&A*, 468, 731
- Józsa, G. I. G. 2007, *A&A*, 468, 903
- Kahn, F. D. 1994, *Ap&SS*, 216, 325
- Kalberla, P. M. W., & Kerp, J. 2009, *ARA&A*, 47, 27
- Kamphuis, J. J. 1993, *PhD Thesis*, University of Groningen
- Kamphuis, J., & Sancisi, R. 1993, *A&A*, 273, 31
- Kenney, J. D. P., van Gorkom, J. H., & Vollmer, B. 2004, *AJ*, 127, 3361
- Keres, D., Katz, N., Weinberg, D. H., & Davé, R. 2005, *MNRAS*, 363, 2
- Kereš, D., Katz, N., Fardal, M., Davé, R., & Weinberg, D. H. 2009a, *MNRAS*, 395, 160
- Kereš, D., Katz, N., Davé, R., Fardal, M., & Weinberg, D. H. 2009b, *MNRAS*, 396, 2332
- Kerr, F. J. 1969, *ARA&A*, 7, 39
- Kennicutt, R. C., Jr. 1989, *ApJ*, 344, 685
- Kennicutt, R. C., Jr. 1998, *ARA&A*, 36, 189
- Kennicutt, R. C., Jr., et al. 2003, *PASP*, 115, 928
- Koribalski, B. S., et al. 2004, *AJ*, 128, 16 (HIPASS)
- Kregel, M., & van der Kruit, P. C. 2005, *MNRAS*, 358, 481
- Lah, P., et al. 2007, *MNRAS*, 376, 1357
- Leroy, A. K., Walter, F., Brinks, E., Bigiel, F., de Blok, W. J. G., Madore, B., & Thornley, M. D. 2008, *AJ*, 136, 2782 (HERACLES) (THINGS)
- Leroy, A. K., et al. 2009, *AJ*, 137, 4670 (HERACLES) (THINGS)
- Leroy, A. K., et al. 2011a, *ApJ*, 737, 12 (HERACLES) (THINGS)
- Leroy, A. K., Walter, F., Schruba, A., Bigiel, F., Foyle, K., & HERACLES Team 2011b, *AAS*, 43, #246.14
- Leroy, A. K., Walter, F., Schruba, A., & HERACLES Collaboration 2012, *AAS*, 219, #346.03
- Levine, E. S., Blitz, L., & Heiles, C. 2006, *ApJ*, 643, 881
- Liszt, H. S., Pety, J., & Lucas, R. 2010, *A&A*, 518, A45
- Madau, P., Pozzetti, L., & Dickinson, M. 1998, *ApJ*, 498, 106
- Madore, B. F., van den Bergh, S., & Rogstad, D. H. 1974, *ApJ*, 191, 317
- Marasco, A., & Fraternali, F. 2011, *A&A*, 525, A134
- Marasco, A., Fraternali, F., & Binney, J. J. 2012, *MNRAS*, 419, 1107
- Marinacci, F., Binney, J., Fraternali, F., Nipoti, C., Ciotti, L., & Londrillo, P. 2010, *MNRAS*, 404, 1464
- Martin, C. L., & Kennicutt, R. C., Jr. 2001, *ApJ*, 555, 301
- Martinez-Delgado, D., et al. 2010, *AJ*, 140, 962

- Meyer, M. J., et al. 2004, *MNRAS*, 350, 1195 (HIPASS)
- Muller, C. A., & Oort, J. H. 1951, *Nature*, 168, 357
- Newton, K. 1980, *MNRAS*, 190, 689
- Noordermeer, E., van der Hulst, J. M., Sancisi, R., Swaters, R. A., & van Albada, T. S. 2005, *A&A*, 442, 137 [WHISP]
- Norman, C. A., & Ikeuchi, S. 1989, *ApJ*, 345, 372
- O'Brien, J. C., Freeman, K. C., & van der Kruit, P. C. 2010, *A&A*, 515, A62 and A63
- Olling, R. P. 1996, *AJ*, 112, 457
- Oosterloo, T., & van Gorkom, J. 2005, *A&A*, 437, L19
- Oosterloo, T., Fraternali, F., & Sancisi, R. 2007a, *AJ*, 134, 1019
- Oosterloo, T. A., et al. 2007b, *NewAR*, 51, 8
- Oosterloo, T. A., Morganti, R., Sadler, E. M., van der Hulst, T., & Serra, P. 2007c, *A&A*, 465, 787
- Oosterloo, T. A., et al. 2010a, *MNRAS*, 409, 500
- Oosterloo, T., Verheijen, M., & van Cappellen, W. 2010b, *PoS (ISKAF2010)* 043 http://pos.sissa.it/archive/conferences/112/043/ISKAF2010_043.pdf
- Ott, J., Skillman, E., Dalcanton, J., Walter, F., Stilp, A., Koribalski, B., West, A., & Warren, S. 2008, *AIPC*, 1035, 105 (VLA-ANGST)
- Pawsey, J. L. 1951, *Nature*, 168, 358
- Putman, M. E., Staveley-Smith, L., Freeman, K. C., Gibson, B. K., & Barnes, D. G. 2003, *ApJ*, 586, 170
- Raimond, E., & Volders, L. M. J. S. 1957, *BAN*, 14, 19
- Rand, R. J., Kulkarni, S. R., & Hester, J. J. 1990, *ApJ*, 352, L1
- Regan, M. W., Thornley, M. D., Helfer, T. T., Sheth, K., Wong, T., Vogel, S. N., Blitz, L., & Bock, D. C.-J. 2001, *ApJ*, 561, 218 (BIMA-SONG)
- Reynolds, R. J. 1971, PhD Thesis, University of Wisconsin
- Reynolds, R. J., Scherb, F., & Roesler, F. L. 1973, *ApJ*, 185, 869
- Rickard, L. J., Palmer, P., Morris, M., Zuckerman, B., & Turner, B. E. 1975a, *BAAAS*, 7, 253
- Rickard, L. J., Palmer, P., Morris, M., Zuckerman, B., & Turner, B. E. 1975b, *BAAAS*, 7, 529
- Roberts, M. S. 1963, *ARA&A*, 1, 149
- Roberts, M. S. 1975, *Stars and Stellar Systems*, Vol. IX (Chicago: University of Chicago Press), 309
- Roberts, M. S., & Haynes, M. P. 1994, *ARA&A*, 32, 115
- Rogstad, D. H., & Shostak, G. S. 1971, *A&A*, 13, 99
- Rosen, A., & Bregman, J. N. 1995, *ApJ*, 440, 634
- Roychowdhury, S., Chengalur, J. N., Begum, A., & Karachentsev, I. D. 2009, *MNRAS*, 397, 1435 (FIGGS)
- Roychowdhury, S., Chengalur, J. N., Begum, A., & Karachentsev, I. D. 2010, *MNRAS*, 404, L60 (FIGGS)
- Rupen, M. P. 1991, *AJ*, 102, 48
- Sancisi, R., & Allen, R. J. 1979, *A&A*, 74, 73
- Sancisi, R., Fraternali, F., Oosterloo, T., & van der Hulst, T. 2008, *A&AR*, 15, 189
- Sanders, R. H. 2010, *The Dark Matter Problem* (Cambridge University Press), ISBN:9780521113014
- Sanduleak, N. 1969, *AJ*, 74, 47
- Savage, B. D., & de Boer, K. S. 1979, *ApJ*, 230, L77
- Schaap, W. E., Sancisi, R., & Swaters, R. A. 2000, *A&A*, 356, 49L
- Schaye, J. 2004, *ApJ*, 609, 667
- Schruba, A., et al. 2011, *AJ*, 142, 37
- Schmidt, M. 1959, *ApJ*, 129, 243
- Serra, P., et al. 2012, *MNRAS*, 422, 1835 (ATLAS3D)
- Shetty, R., Glover, S. C., Dullemond, C. P., Ostriker, E. C., Harris, A. I., & Klessen, R. S. 2011, *MNRAS*, 415, 3253
- Shetty, R., Glover, S. C., Dullemond, C. P., & Klessen, R. S. 2011, *MNRAS*, 412, 1686
- Shull, J. M., & Beckwith, S. 1982, *ARA&A*, 20, 163
- Skillman, E. D. 1987, *NASCP*, 2466, 263
- Solanes, J. M., Manrique, A., García-Gómez, C., González-Casado, G., Giovanelli, R., & Haynes, M. P. 2001, *ApJ*, 548, 97
- Springel, V., Di Matteo, T., & Hernquist, L. 2005, *MNRAS*, 361, 776
- Stein, W. A., & Soifer, B. T. 1983, *ARA&A*, 21, 177
- Swaters, R. A., Sancisi, R., & van der Hulst, J. M. 1997, *ApJ*, 491, 140
- Swaters, R. A., van Albada, T. S., van der Hulst, J. M., & Sancisi, R. 2002, *A&A*, 390, 829 (WHISP)
- Taylor, E. N., & Webster, R. L. 2005, *ApJ*, 634, 1067
- Thilker, D. A., et al. 2005, *ApJ*, 619, L79
- Thilker, D. A., et al. 2007, *ApJS*, 173, 538
- Toribio, M. C., Solanes, J. M., Giovanelli, R., Haynes, M. P., & Martin, A. M. 2011, *ApJ*, 732, 93 [ALFALFA]
- Tosa, M., & Hamajima, K. 1975, *PASJ*, 27, 501
- Valentijn, E. A., & van der Werf, P. P. 1999, *ApJ*, 522, L29
- Valentijn, E. A., van der Werf, P. P., de Graauw, T., & de Jong, T. 1996, *A&A*, 315, L145
- van de Hulst, H. C. 1945, *Ned. Tijdschr. voor Natuurkunde*, 11, 201
- van der Hulst, J. M., & Sancisi, R. 1988, *AJ*, 95, 1354
- van der Hulst, J. M., Skillman, E. D., Smith, T. R., Bothun, G. D., McGaugh, S. S., & de Blok, W. J. G. 1993, *AJ*, 106, 548
- van der Hulst, J. M., van Albada, T. S., & Sancisi, R. 2001, *ASPC*, 240, 451 (WHISP)
- van der Kruit, P. C., & Freeman, K. C. 2011, *ARA&A*, 49, 301
- van de Voort, F., Schaye, J., Booth, C. M., & Dalla Vecchia, C. 2011, *MNRAS*, 415, 2782
- van Eymeren, J., Jütte, E., Jog, C. J., Stein, Y., & Dettmar, R.-J. 2011a, *A&A*, 530, A29

- van Eymeren, J., Jütte, E., Jog, C. J., Stein, Y., & Dettmar, R.-J. 2011b, *A&A*, 530, A30
- van Gorkom, J. 2008, *AIPC*, 1035, 24
- van Gorkom, J. 2011, *IAU Symp.*, 277, 41
- Verheijen, M. A. W., Oosterloo, T. A., van Cappellen, W. A., Bakker, L., Ivashina, M. V., & van der Hulst, J. M. 2008, *AIPC*, 1035, 265
- Verheijen, M., Oosterloo, T., Heald, G., & van Cappellen, W. 2009, *PoS (PRA2009)* 089, <http://pos.sissa.it/cgi-bin/reader/conf.cgi?confid=89>
- Volders, L. M. J. S. 1959, *BAN*, 14, 323
- Volders, L. M. J. S., & Högbom, J. A. 1961, *BAN*, 15, 307
- Walter, F., Brinks, E., de Blok, W. J. G., Bigiel, F., Kennicutt, R. C., Jr., Thornley, M. D., & Leroy, A. 2008, *AJ*, 136, 2563 (THINGS)
- Walterbos, R. A. M., & Braun, R. 1996, *The Minnesota lectures on extragalactic neutral hydrogen*. ASPC, 106, 1
- Warmels, R. H. 1988, *A&AS*, 72, 19, 17, and 427
- Westmeier, T., & Johnston, S. 2010, *PoS (ISKAF2010)* 056, http://pos.sissa.it/archive/conferences/112/056/ISKAF2010_056.pdf
- Wilson, C. D. 1995, *ApJ*, 447, 616
- Wilson, R. W., Jefferts, K. B., & Penzias, A. A. 1970, *ApJ*, 161, L43
- Wright, M. C. H., Warner, P. J., & Baldwin, J. E. 1972, *MNRAS*, 155, 337
- Young, J. S., & Scoville, N. Z. 1991, *ARA&A*, 29, 581
- Zwaan, M. A., et al. 2004, *MNRAS*, 350, 1210 (HIPASS)